Lichen-associated bacteria transform antibacterial usnic acid to products of lower antibiotic activity

Alba Noël, Alexandre Garnier, Mélanie Clément, Isabelle Rouaud, Aurélie Sauvager, Latifa Bousarghin, P Vasquez-Ocmin, Alexandre Maciuk, Sophie Tomasi

Graphical abstract:

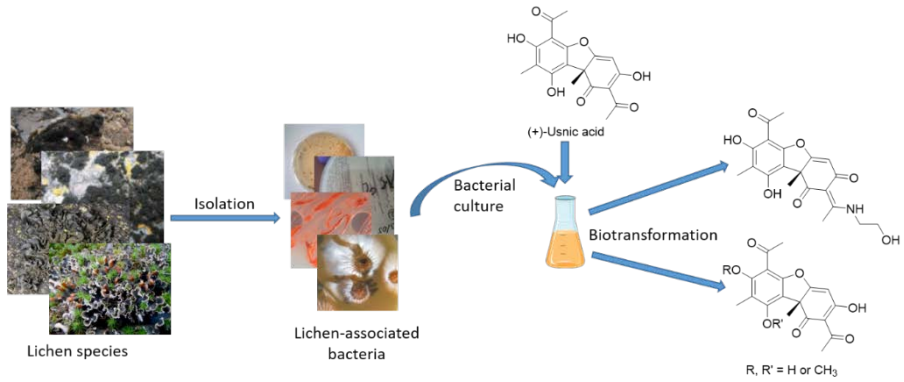

(+)-Usnic acid derivatives identified from culture broth of lichen-associated bacteria enriched with usnic acid.

Lichen-associated bacteria transform antibacterial usnic acid to products of lower antibiotic activity

Alba Noël[a], Alexandre Garnier[a], Mélanie Clément[a], Isabelle Rouaud[a], Aurelie Sauvager[a], Latifa Bousarghin[b], Pedro Vásquez-Ocmín[c], Alexandre Maciuk[c], Sophie Tomasi*[a]

[a] Univ Rennes, CNRS, Institut des Sciences Chimiques de Rennes – UMR 6226, F-35000 Rennes, France

[b] INSERM, Univ. Rennes, INRA, CHU Rennes, Nutrition Metabolisms and Cancer (NuMeCan), UMR-1241, Biosit, MRic/ISFR, Rennes, France

[c] Université Paris-Saclay, CNRS, BioCIS, 92290, Châtenay-Malabry, France.

***Corresponding Author:** Professor Sophie Tomasi, COrInt, UMR CNRS ISCR 6226, UFR Sciences Pharmaceutiques et Biologiques, 2 Av. du Professeur Léon Bernard, 35043 Rennes, France. +332 23 23 48 17

E-mail: sophie.tomasi@univ-rennes1.fr

Abstract:

Lichens are specific symbiotic organisms harboring various microorganisms in addition to the two classic partners (algae or cyanobacterium and fungus). Although lichens produce many antibiotic compounds such as (+)-usnic acid, their associated microorganisms possess the ability to colonize an environment where antibiosis exists. Here, we have studied the behavior of several lichen-associated bacterial strains in the presence of (+)-usnic acid, a known antibiotic lichen compound. The effect of this compound was firstly evaluated on the growth and metabolism of three bacteria, thus showing its ability to inhibit Gram-positive bacteria. This inhibition was not thwarted with the usnic acid producer strain *Streptomyces cyaneofuscatus*. The biotransformation of this lichen metabolite was also studied. An ethanolamine derivative of (+)-usnic acid with low antibiotic activity was highlighted with chemical profiling, using HPLC-UV combined with low resolution mass spectrometry. These findings highlight the way in which some strains develop resistance mechanisms. A methylated derivative of (+)-usnic acid was annotated using the molecular networking method, thus showing the interest of this computer-based approach in biotransformation studies.

Keywords: *Streptomyces cyaneofuscatus*; *Nocardia* sp.; *Mabikibacter ruber; Bacillus weihenstephenensis;* Actinobacteria; Alphaproteobacteria; Firmicutes; Biotransformation; Molecular networking; Usnic acid derivatives.

1. Introduction

Lichens are well known to produce specific compounds with a unique structure for example, dibenzofuranes, depsides, depsidones, etc. Most of these compounds have exhibited various biological activities (Calcott et al.2018), mainly in the field of photoprotection but also as cytotoxic, antibacterial, or antifungal agents. It is now well established that lichens are complex ecosystems, containing various associated fungi, bacteria and other microscopic organisms, living in permanent association with the lichen thallus (Hawksworth and Grube, 2020). Consequently, their microflora are in contact with potential toxic metabolites. The role of associated bacteria inside the lichen network is still unknown. However some involvement of these microorganisms in defending lichen against intrinsic or extrinsic factors has been previously described, together with both a degradation of the lichen thallus and the nitrogen supply (Grube et al., 2015; Grube and Berg, 2009). The microbiome of some lichens has been localized by FISH (Fluorescence *In Situ* Hybridization) and CLSM (Confocal Laser Scanning Microscopy) mainly on both the upper and lower cortex of the lichen *Lobaria*

pulmonaria (L.) Hoffm. (Grube et al., 2015) and on the inner surface of the cylindrical podetia of *Cladonia arbuscula* (Wallr.) Flot. (Cardinale et al., 2008). These lichen-associated bacteria are of great interest for the chemical diversity of compounds produced and for their biotechnological potential (Bates et al., 2011; Nahar et al., 2019; Suzuki et al., 2016; Zheng et al., 2019). We studied here the behavior of lichen-associated bacteria in the presence of a specific active lichen compound, namely (+)-usnic acid (UA). UA has been reported as an antibacterial agent against Gram-positive bacteria (Calcott et al., 2018; Maciąg-Dorszyńska et al., 2014). Gram-positive or -negative bacteria have nevertheless been isolated from lichens producing UA. Fewer bacteria were thus present on the peripheral parts of the *C. arbuscula* thallus, close to the crystallized UA deposits (Cardinale et al., 2008), showing that these strains can adapt to chemical stress.

Our main goal herein is to study the effect of UA on the bacterial growth and metabolism of different bacterial strains isolated from lichens. The strains studied belong to the three main bacterial phyla isolated from various lichens: Actinobacteria, Alphaproteobacteria and Firmicutes (Parrot et al., 2015a). The Alphaproteobacterium selected was *Mabikibacter ruber* (also labeled MOLA1416), a Gram-negative strain previously isolated from the lichen *Lichina pygmaea* (Lightf.) C. Agardh, and its chemical composition was described by Parrot et al., 2018. Among the two Actinobacteria studied, *Nocardia* sp was isolated from the lichen *Lathagrium auriforme* (With.) Otálora, P. M. Jørg. & Wedin, and its chemical composition was previously described (Noël et al., 2017). The second strain, *Streptomyces cyaneofuscatus* (MOLA1488), isolated from *Lichina confinis* (O.F. Müll.) C. Agardh, was selected as a producer of UA (Parrot et al., 2016). The Firmicutes strain studied herein was isolated from the lichen *Peltigera hymenina* (Ach.) Delise and identified as *Bacillus weihenstephanensis* (data not published).

In the first part of this work, we studied the bacterial growth of three lichen-associated strains (*Nocardia* sp, *S. cyaneofuscatus*, *M*. *ruber*) after UA supplementation. The chemical profiles of the culture supernatants were studied to determine the potential impact of the added compound on bacterial metabolism.

In the second part, a biotransformation study was carried out to highlight the means used by bacteria to eliminate a potential toxic compound. We studied the UA biotransformation ability of three lichen-associated bacteria, namely Firmicutes *B. weihenstephanensis,* Alphaproteobacterium MOLA1416 and Actinobacterium *Nocardia* sp. These strains were incubated with three different concentrations of UA (0.01 mg/mL, 0.1 mg/mL and 0.5 mg/mL) along with untreated cultures as controls. The method used was based on the resting cell method, commonly used for biotransformation studies (Baqueiro-Peña et al., 2019; Jackson et al., 2019; Luziatelli et al., 2019).

Initial HPLC analysis highlighted the compounds produced only in the presence of UA. Next, to identify biotransformation derivatives, all the extracts underwent LC-MS/MS and the data were processed using a workflow combining preprocessing with MZmine 2 (Pluskal et al., 2010) and molecular networking analysis with the GNPS tool (Wang et al., 2016). This MS/MS-based computational approach compares all the fragmentation spectra with each other and with databases. All spectra with similar fragmentation patterns are gathered in clusters and each cluster includes compounds belonging to the same structural family. The use of this tool in biotransformation studies allows the rapid identification of bioconversed derivatives by spotting the corresponding cluster as it has already been performed for drug metabolites (Robertson et al., 2015). The recent development of a database for lichen metabolites (Olivier-Jimenez et al., 2019) is a complementary tool for our study to potentially detect derivative compounds with a structure similar to known lichen compounds.

2. Results

2.1. Effects of (+)-usnic acid on lichen-associated bacteria

2.1.1 Effects on bacterial growth

The antibacterial effect of (+)-usnic acid (UA) was evaluated at 0.1 mg/mL on three bacterial strains (*Nocardia* sp, *S. cyaneofuscatus*, *M*. *ruber*) isolated from various lichens. The lichen compound UA was added to the bacterial broth at the beginning of the culture and the optical density was measured at 620 nm to establish the bacterial growth curve. Cell viability was also monitored using MTT (3-(4, 5-dimethylthiazolyl-2)-2,5-diphenyltetrazolium bromide) assay.

Fig. 1. Monitoring of the bacterial growth over 15 days (D0 to D15) by measuring optical density (log OD (optical density), gray curve) and cell viability (%) using MTT assay (blue curve) compared to untreated culture (orange curve). A) *Nocardia* sp., B) *S. cyaneofuscatus*, C) *M. ruber*.

UA inhibits the bacterial growth of the two Gram positive strains *Nocardia* sp. and *S. cyaneofuscatus* (Fig. 1.A and 1.B). The growth of the Gram negative strain *M*. *ruber* is slightly delayed in the presence of UA but no inhibition is observed (Figure 1.C). These results confirm the specific antibacterial activity of UA on Gram-positive bacteria (Lauterwein et al., 1995).

2.1.2 Effects on bacterial metabolism

The culture broth of the three lichen-associated bacteria was harvested at the beginning of the stationary phase of bacterial growth and after 7 days of stationary phase (following the bacterial growth curve measured). After extraction, the metabolic profiles of each sample were analyzed by HPLC and compared with those of the untreated samples. Metabolism modification was highlighted on chromatograms (Figures 2-4). To target the (+)-usnic acid derivatives, UV profiles were observed at a wavelength of 272 nm (Figure 2-4). This value was selected according to the maximal UV absorption of the dibenzofurane compounds classically described between 256 and 274 nm (Millot et al., 2016) which are close to those of UA (see S1).

After 7 days of stationary phase growth, cultures of *M. ruber* show the presence of a few additional metabolites (between 30 and 35 min) not detected in untreated cultures (Fig. 2).

Fig. 2. HPLC chromatograms of *M. ruber* cultures with or without UA. A) At the beginning of the stationary phase of bacterial growth; B) After 7 days of stationary phase. Compounds circled in red appear only in the culture with UA.

In the same way, UA induces the production of several compounds (eluted between 25 and 35 min) by the *Nocardia* sp. Strain. These compounds are absent in the culture medium (Fig. 3). Furthermore, the presence of UA does not affect the metabolism of compounds eluted earlier (0-20 min). No change is observed after 7 more days of *Nocardia* sp. culture (Fig. 3B).

Fig. 3. HPLC chromatograms of *Nocardia* sp. culture with or without UA. A) At the beginning of the stationary phase of the bacterial growth; B) After 7 days of stationary phase. Compounds circled in red appear only in the culture with UA.

The second Gram-positive strain *S. cyaneofuscatus* exhibits a significant variation of its chemical profile in the presence of UA compared with those of untreated cultures (Fig. 4). Several compounds are not produced, probably due to growth inhibition. The production of the diketopiperazine cyclo-(*L*-Leu-*L*-Pro), a major compound eluting at 20.8 min (Parrot et al., 2016), is completely inhibited after UA treatment. Even after 7 days of stationary phase growth, these compounds are still not produced in the presence of UA.

Fig. 4. HPLC chromatograms of *S. cyaneofuscatus* cultures with or without UA: A) At the beginning of the stationary phase of bacterial growth; B) After 7 days of stationary phase. Circled in blue: compounds inhibited in the presence of UA, circled in orange: compounds more concentrated in the presence of UA, circled in red: UA.

Conversely, some compounds appear in the presence of UA. The compound eluting at 13.3 min (Fig. 4) was determined using low resolution mass spectrometry (electrospray ionisation (ESI) in positive mode) at *m/z* 268. This compound was identified as a component of the medium which is not consumed by the inhibited strain. The other two compounds eluting at 26.4 and 31.6 min respectively were analyzed by mass spectrometry in negative mode and correspond to two ions at *m/z* 333 and *m/z* 359 respectively. After 7 days of stationary phase, these two compounds are no longer detectable using our HPLC conditions. These molecules could putatively either derive from UA after biotransformation by the bacterial strain or be induced by the presence of UA. Nevertheless, no valid hypothesis of structure could be proposed using low resolution mass spectrometry.

2.2. Biotransformation of (+)-usnic acid

The resting cell method was performed with three different lichen-associated bacteria (*M*. *ruber*, *Bacillus weihenstephenensis* and *Nocardia* sp.) belonging to the three most representative phyla on lichen: Alphaproteobacteria, Firmicutes and Actinobacteria. We did not select *S*. *cyaneofuscatus* as it is already known to produce UA.

2.2.1. Compounds highlighted by chemical profiling

The chemical profiles of the bacterial extracts obtained with or without UA were compared using HPLC-UV thus highlighting the compounds produced specifically after UA addition. To target the UA derivatives, UV profiles were observed at a wavelength of 272 nm (Figure 7). Only ten additional peaks appeared on HPLC chromatograms of the three bacterial cultures treated by UA (Table 1).

Table 1 Additional peaks detected only in cultures treated with UA at different concentrations (0.01 to 0.5 mg/mL).

According to the results depicted in Table 1, UA seems to be metabolized in different ways depending on the bacterial strain. Some compounds are commonly produced by the three strains such as the compound **E** and the others are produced by one or two bacteria. One of these compounds labeled **H**, found in all extracts of *M*. *ruber* , in extracts of *Nocardia* sp. with UA at 0.5 mg/mL and in extracts of *B. weihenstephanensis* with UA at 0.01 mg/mL (Fig. 5), was identified by LC-HRMS in negative mode. The analysis gave a molecular peak at *m/z* 386.1226 corresponding to a molecular formula of $C_{20}H_{20}O_7N$. This compound was identified as an ethanolamine derivative of UA,

which is close to derivatives previously obtained synthetically by our group (Bazin et al., 2008) (Fig. 6).

Fig. 5. Comparison of HPLC chromatograms of *B. weihenstephanensis* extracts with UA at 0.01 mg/mL after 1 day of culture (blue), 9 days of culture (black) and without UA after 9 days of culture (red).

Fig. 6. UA and the ethanolamine **H** derivative obtained after biotransformation

2.2.2. Synthesis and activity of ethanolamine – usnic acid conjugate **H**

For a better understanding of the production of the compound **H**, we synthesized this compound with a 78% yield using our approach as previously described (Bazin et al., 2008). The structure of compound **H** was thus confirmed in comparison to this standard (see S2 and S3). We also evaluated its putative antibacterial effect against two Gram-negative and four Gram-positive pathogenic bacterial strains and compared its activity to those of UA (Table 2). While UA is active against all the Gram-positive strains with the Minimal Inhibition Concentration (MIC) ranging between 1.56 and 6.25 µg/mL, compound **H** is inactive against all the pathogenic strains tested with an MIC between 25 and 50 µg/mL. This indicates that *M*. *ruber*, *Nocardia* sp. and *B. weihenstephensis* have the ability to convert UA into a less active compound.

Table 2 Antibacterial evaluation of UA and compound **H** against six pathogenic human bacterial strains

2.2.3. Compounds highlighted by molecular networking

We analyzed the extracts using LC/MS-MS in order to detect compounds derived from UA after its biotransformation by our strains. The network was enriched with various lichen compounds as standard as variolaric acid, gyrophoric acid, orsellinic acid, stictic acid, pannaric acid, atranol, methyl-β-orcinol carboxylate (MOC), atranorin and (+)-usnic acid. All the data obtained were then processed with MZmine 2 and the GNPS platform to build molecular networks. The recent completion of the GNPS tool with a lichen compound database by Olivier-Jimenez et al., 2019, allowed us to compare our data with various lichen compounds. Among our nine standards used, only stictic acid and orsellinic acid did not match the LDB, and gyrophoric acid matched lecanoric acid, a lichen compound with very close fragmentation. These results validate our data analysis and reprocessing methods.

We focused on the network corresponding to the UA and potential derivatives exhibiting a close fragmentation pathway. The other lichen compounds were represented either in self-loop or clustered with control compounds, meaning that the compounds putatively resulting from biotransformation of UA do not possess a structure close to these standards (Fig. 7).

Fig. 7. Molecular networking results from GNPS visualized with Cytoscape. Inset: cluster of UA and derivatives with close fragmentation pathway (*m/z* 357.12: compound **K**, *m/z* 389.104: compound **L**) and self-loop of compound **H** (at *m/z* 386.139).

Compound **H** is not included in the UA cluster, as one of the setting parameters for GNPS analysis was 6 matched peaks to create a network. In fact, the fragmentation patterns of this metabolite and those of UA only share two fragments (*m/z* 259 and 231) as we can see in Fig. 8.

Fig. 8. Fragmentation patterns in negative mode of A) compound **H** and B) UA; common fragments are highlighted in orange.

Two compounds, **K** and **L** at *m/z* 357 and *m/z* 389 are clustered with UA under our conditions (Fig. 7 and see MS/MS fragmentation patterns in S4). Thanks to the exact mass of the compound at 357 (*m/z* 357.1135) and its fragmentation pattern, the structural hypothesis has been established. Compound **K** appears to be a methylated derivative of UA and a proposed fragmentation pattern of one possible isomer of this compound is depicted in Fig. 9. Compound **L** shares the same fragments as UA (at *m/z* 259.07, 231.07 and 83.01) and shows four supplementary fragments (at *m/z* 342.09, 314.06, 273.08 and 97.03). According to the mass difference of 46 with UA, compound **L** could be derived from UA after the addition of formate or ethanol moiety. The fragment ion at *m/z* 345 is in accordance with these hypotheses.

Fig. 9. Fragmentation pattern proposed for one possible isomer of the methylated usnic acid **K**

3. Discussion

We have highlighted the effects of UA on bacterial growth and metabolism. After supplementation in cultures, UA strongly and specifically inhibits the growth of Gram-positive bacteria, as previously demonstrated (Lauterwein et al., 1995). In parallel, the Gram-positive strain *Nocardia* sp. exhibits an increase in the production of unidentified compounds (eluted between 25-35 min) in comparison with the untreated culture. These compounds could be either UA derivatives metabolized in an

attempt to eliminate this toxic compound or signal molecules involved in bacterial death (Rice and Bayles, 2008).

Growth and metabolism inhibition was also shown on *S. cyaneofuscatus* even though this strain is able to produce UA (Parrot et al., 2016). This was highlighted by the non-consumption of components of the culture medium and this time by a decrease in bacterial production. Because of the presence of a toxic compound, bacteria could save resources by limiting non-vital function and by stopping the production of various compounds. The inhibition of bacterial growth could thus lead to a decrease in the production of quorum sensing signal molecules. In fact, diketopiperazines are well known for being signal molecules for quorum sensing (Martins and Carvalho, 2007). Indeed, the inhibition of cyclo-(*L*-Leu-*L*-Pro) production could be explained by the influence of UA on quorum sensing as it has already been described by Francolini et al., 2004, during the formation of biofilm of *Staphylococcus aureus*. It appears that no resistance is developed by *S*. *cyaneofuscatus* following the acquisition of production capacity.

The biosynthetic UA gene cluster, belonging to the polyketide synthase family (PKS), should be acquired by the bacterial strain using horizontal transfer as it has been already described for many PKS clusters (Schmitt and Lumbsch, 2009). As the toxic compound was added to the medium at the very beginning of the bacterial culture, the production of the antibiotic, which occurred during the stationary phase of bacterial growth, was not primed by the bacterial strain. Likewise, bacterial resistance to antibiotics had been reported as non-effective before the beginning of production of the compound (Martin and Demain, 1980). Thus, it was reported that the bacterial resistance of the *Streptomyces* strain to the PKS antibiotic compound, actinorhodin, was not activated by the final product but by a precursor of its biosynthesis (Tahlan et al., 2008). This strain was only sensitive to an exogenous addition of this antibiotic when this occurred before the beginning of biosynthesis. Furthermore, the effects of UA on bacterial growth were established at 0.1 mg/mL which is significantly higher than the level of UA production by *S. cyaneofuscatus* (0.04 µg/mL) (Parrot et al., 2016). As demonstrated by Goh et al., 2002, sub-inhibitory concentrations of antibiotics may have several beneficial effects on microorganisms, thus explaining the ecological benefits of this compound for the bacterial strain. The production of UA could finally be a way to regulate bacterial proliferation inside the lichen micro-ecosystem, and be a selective advantage by producing a toxic component for other bacterial partners.

By contrast, the metabolism of the Gram-negative strain *M*. *ruber* was only slightly affected by the presence of UA in culture broth, which corroborates previous papers indicating the resistance of

Gram-negative bacteria due to a lack of membrane permeability for this compound (Luzina and Salakhutdinov, 2018).

The biotransformation study revealed the detoxification potential of the bacterial strains on the lichen compounds. In fact, we have highlighted the production of some UA derivatives, one of which, the ethanolamine-UA conjugate **H**, exhibited a lower antibiotic effect that the parent compound. The addition of an ethanolamine moiety to a natural product has already been reported, such as for sesquiterpene ilimaquinone biotransformed by a marine fungus (Boufridi et al., 2016). It is worth noting that ethanolamine metabolism has been already reported in mammalian gut as a carbon and nitrogen source for microbiota (Zhou et al., 2017). Moreover, a previous report revealed the capabilities of UA degradation by the stomach microbiota of reindeer in less toxic compounds (Sundset et al., 2010). Here, we have shown that the lichen-associated microbiota are also able to degrade UA, including bacteria isolated from lichens non-producers of UA. This highlights a putative means for lichen-associated bacterial strains to develop resistance against the antibiotic lichen metabolite present in their environmental ecosystem. It is interesting to note that *S*. *cyaneofuscatus*, producer of UA and sensitive to this antibiotic, was also isolated from *L*. *confinis*, the host of *M. ruber*, and from *R. fuciformis*, two other littoral lichens (Parrot et al., 2015a) found in the same environment as *L*. *pygmaea*. *R. fuciformis*, from which Nocardia-like strains (*Nocardioides mesophilus*) (Parrot et al., 2015a) were isolated, is a well-known lichen producer of orsellinic derivatives (montagnetol, erythrin, etc.) (Parrot et al., 2015b). These derivatives possess the same biosynthetic tetraketide precursor as UA (Taguchi et al., 1969). Finally, one of the bacterial strains used in this study, B. *weihenstephanensis*, has also been isolated from *Cladonia coccifera*, a UA-producing lichen (Cardinale et al., 2006). As UA is mainly present in the cortical area of the lichen thallus, as described by Le Pogam et al., 2016 for *Ophioparma ventosa,* and such as reported for the main population of the microbiota (Cardinale et al., 2008; Grube et al., 2015), microorganisms are probably affected by a low concentration of UA. This explains their selective advantage in developing a resistance mechanism. All these findings might explain how these strains have acquired UA degradation capability.

4. Conclusion

The importance of the known compound, UA, for lichen-symbiotic organisms, has been previously highlighted, due to its ability to regulate the growth of Gram-positive bacteria, to be a natural herbicide, and to preserve lichens as ultraviolet absorber (Cocchietto et al., 2002). Our work confirms

the antibacterial activity of UA on Gram-positive bacteria associated with lichens. We also demonstrate that this lichen compound modifies the metabolism of the strains cultivated in its presence. Compounds from medium were less consumed by the bacteria, and specialized metabolites such as diketopiperazines were produced to a lesser extent, in accordance with bacterial growth inhibition. Interestingly, several compounds appeared only in the presence of UA in culture broth. Some of these compounds have been identified as UA derivatives either by chemical profiling or by molecular networking. The detection of an ethanolamine and a methylated derivative of UA illustrates the ability of the lichen-associated bacteria to biotransform toxic compounds into derivatives (as for compound **H**) with less antibiotic properties for some of them. It is also important to note that the highlighted metabolites are produced by Gram-negative and Gram-positive strains, indicating that the metabolism pathways are shared by sensitive and non-sensitive bacteria. These abilities potentially lead sensitive strains to colonize environments surrounded by antibacterial compounds such as lichen thallus. These experiments therefore have given some insight into unraveling the relationships between the primary partners of lichens (photobionts and mycobionts) and the associated bacteria. This work also demonstrates the interest of modern tools such as molecular networking in biotransformation studies, making it possible to rapidly identify derivatives of the compound studied.

5. Experimental section

5.1. Chemicals and reagents

All commercial reagents were purchased from Carlo Erba Reactifs and/or from Sigma Aldrich (Val de Reuil, France and St Quentin Fallavier, France). (+)-UA was purchased from Aldrich. For chromatographic analysis, HPLC and LC/MS grade water was obtained using an EasyPure (Barnstead, USA) water purification system. Deuterated solvents were purchased from Euriso-top (Gif-sur-Yvette, France).

5.2. Microorganisms

Streptomyces cyaneofuscatus (MOLA1488) (Actinobacterium) and *Mabikibacter ruber* (MOLA1416) (Alphaproteobacterium) were isolated respectively from the lichens *Lichina confinis* (O.F. Müll.) C. Agardh and *Lichina pygmaea* (Lightf.) C. Agardh collected in Erquy (Northwest of Rennes, France, 48°37’45’’ N, 02°28’30’’ W) in April 2012 (Parrot et al., 2015a). To identify the strains, their 16S rRNA genes were sequenced using the dideoxy termination (Sanger) sequencing as previously described (Parrot et al., 2015a). Comparison with sequences in the EzTaxon type strain database (Kim et al.,

2012) revealed that the closest phylogenetic neighbor of the strain MOLA1488 was *Streptomyces cyaneofuscatus* with 100% sequence identity and for MOLA1416 it was *Mabikibacter ruber* with 100% sequence identity (re-identified in July 2018 by Laurent Intertaglia, Platform Bio2mar, Banyuls/Mer, France, in comparison to a new species described in [Choi et al., 2017]). The strains were cryopreserved at –80 °C in 50% v/v glycerol or 5% v/v DMSO after growth in either Luria broth (LB) for MOLA1488 or marine broth medium (MB) for MOLA1416 (Difco®) (Banyuls/Mer collection, references: MOLA1488 and MOLA1416).

Nocardia sp. (Actinobacterium) was isolated from the lichen *Lathagrium auriforme* (With.) Otálora, P. M. Jørg. & Wedin collected in Kesselfallklamm (Austria, 47°12'21.26" N, 15°23'57.27" E) in November 2012. The strain was identified by sequencing its 16S rRNA gene using Sanger sequencing (Parrot et al., 2015a). These data were compared with sequences in the EzTaxon type strain database, and showed that the close phylogenetic neighbor of the strain was *Nocardia ignorata* DQ659907 at 98.59% sequence identity. A second sequencing session performed in 2017 by L. Intertaglia revealed 100% sequence identity with *Nocardia soli*, *N. salmonicida* and *N. cummidelens*. The bacteria were stored after growth in ISP2 medium (International Streptomyces Project 2 medium) (4 g yeast extract [Sigma-Aldrich, St. Louis, MO, USA], 10 g malt extract [Sigma-Aldrich, St. Louis, MO, USA], and 4 g Dextrose [Sigma-Aldrich, St. Louis, Missouri] for 1 L) with 50% v/v glycerol or 5% v/v DMSO at -80°C and referenced as DP94 (COrInt collection).

The *Bacillus weihenstephanensis* strain (Firmicutes) was isolated from *Peltigera hymenina* (Ach.) Delise collected in Huelgoat (Brittany, France, 48°21'57'' N, 3°44'47'' W). The lichen thallus was rinsed with "DNase, RNase and protease-free" water, cut into small pieces and placed in a Petri dish containing TY (Tryptone Yeast) medium with agar. After two weeks of incubation at 25°C, transplantation was performed until a pure colony appeared. The bacterial strain was identified by sequencing its 16S rRNA gene using Sanger sequencing. The comparison of these data sequences in the EzTaxon type strain database showed that the close phylogenetic neighbor of the strain was *B. weihenstephanensis* at 100% sequence identity. The bacteria were stored after growth in TY medium with 50% *v*/*v* glycerol or 5% *v*/*v* DMSO at -80°C.

5.3. Fermentation of the strains and biotransformation study

5.3.1. Culture of the strains in the presence of (+)-usnic acid (supplementation study)

The strains *S. cyaneofuscatus*, *M*. *ruber* and *Nocardia* sp. were inoculated in 30 mL of medium (respectively: LB: peptone 5 g/L [Sigma-Aldrich, St Louis, MO, USA], sodium chloride 5 g/L [Sigma-

Aldrich, St Louis, MO, USA] and yeast extract 3 g/L [Sigma-Aldrich, St Louis, MO, USA]; MAI: Marin broth [Difco® 2216, ThermoFisher, Waltham, MA, USA] supplemented with 5 mg/L sodium iodide; TY medium: tryptone 16 g/L [Sigma-Aldrich, St Louis, MO, USA], yeast extract 10 g/L [Sigma-Aldrich, St Louis, MO, USA] and sodium chloride 5 g/L [Sigma-Aldrich, St Louis, MO, USA]) in 50 mL test tubes. (+)-Usnic acid was previously dissolved in DMSO and added at 0.1 mg/mL in each culture. Untreated cultures were inoculated for each strain without any additive and with DMSO. The cultures were incubated in an orbital shaker (110 rpm) at 25°C and stopped at the beginning of the stationary phase growth or after 7 days of the stationary phase growth.

5.3.2 Monitoring of the bacterial growth

The bacterial growth was monitored daily by measuring the optical density of the cultures in 96-well plates with a microplate photometer (Thermo Scientific Multiskan FC ®) at a wavelength of 620 nm.
The cell viability was also monitored by MTT assay (Millot et al., 2009). Ten µL of MTT were added to 200 µL of culture in 96-well plates and the supernatant was removed after 4h of incubation (37°C). Formazan product was dissolved with 200 µL of DMSO and optical density was measured by microplate photometer at 540 nm. Cell viability was calculated as follows:

% = [(OD_{540} – OD_{540} medium)/(OD_{540} bacteria – OD_{540} medium)] x 100

With: OD_{540}: sample value; OD_{540} medium: medium value; OD_{540} bacteria: value of the control culture without an additive.

5.3.3. Fermentation of the strains for biotransformation study

The strains *M*. *ruber*, *Nocardia* sp. and *B. weihenstephanensis* were inoculated in 30 mL of medium (respectively: MAI: Marine broth [Difco ® 2216, ThermoFisher, Waltham, MA, USA] supplemented with 5 mg/L sodium iodide; TY medium: tryptone 16 g/L, yeast extract 10 g/L and sodium chloride 5 g/L; ISP2 medium: yeast extract 4 g/L [Sigma-Aldrich, St. Louis, MO, USA], malt extract 10 g/L [Sigma-Aldrich, St. Louis, MO, USA], and Dextrose 4 g/L [Sigma-Aldrich, St. Louis, Missouri]) in 50 mL test tubes. Cultures were incubated in an orbital shaker (110 rpm) at 25°C for 7 days.

5.3.4. Biotransformation study

After 7 days of incubation, the test tubes were centrifuged at 3500 rpm, 4°C for 15 min. The culture medium was discarded and a solution of lichen compound previously dissolved in DMSO and in a

final concentration of 0.01, 0.1 or 0.5 mg/mL in 0.5 M sterile phosphate buffer at pH 7 (30 mL) was added to the bacterial pellet. For the control sample, only phosphate buffer was added. The cultures were incubated in an orbital shaker (110 rpm) at 25°C and stopped after 1, 2, 4, 7 and 9 days of culture.

5.4. Sample extraction

The test tubes were centrifuged at 3500 rpm, at 4°C for 15 min. The supernatants were collected and extracted with 2 x 30 mL of ethyl acetate (EtOAc). The organic phase (EtOAc extract) was collected and dried on anhydrous sodium sulfate. This phase was finally evaporated under a vacuum to yield the bacterial extracts used for LC-MS/MS analysis.

5.5. Mass spectrometry analysis

5.5.1. LC/MS analysis

Mass spectrometry analysis was carried out on a HPLC system—Diode Array Detector (LC-DAD) (Shimadzu, Marne La Vallée, France) and a mass spectrometer with a single quadrupole mass analyzer (Advion expression CMS, Ithaca, NY, USA). Ionization was performed by electrospray in negative or positive mode (ESI) for low resolution analysis. A Prevail C18 column (5 µm, 250 x 4.6 mm, GRACE, Columbia, MD, USA) was used for HPLC, and a gradient system was applied: A (0.1% formic acid in water) and B (0.1% formic acid in acetonitrile). The following gradient was applied at a flow rate of 0.8 mL/min in the HPLC system: initial: 100% (A); from 0 to 5 min: 100% (A); from 5 to 35 min: 100% (A)/0% (B) to 0% (A)/100% (B); from 35 to 45 min: 100% B; from 45 to 50 min: 100% (A)/0% (B) to 0% (A)/100% (B); from 50 to 55 min: 100% (A). A 0.2 mL/min split was applied for mass spectrometry. Twenty microliters of samples at 1 mg/mL in MeOH were injected.

5.5.2. High resolution LC-MS/MS data acquisition

LC–MS/MS analyses were performed on a 6530 Accurate-Mass Q-TOF LC/MS instrument (Agilent Technologies) which was equipped with an electrospray ionization interface (ESI). Chromatographic separations were performed on a Sunfire C18 column, 4.6 x 150 mm – 5 µm (Waters). The mobile phase comprised water (0.1 % formic acid) (A) and acetonitrile (B). A stepwise gradient method at a constant flow rate of 0.2 mL/min was used to elute the column under the following conditions: 2–100% B (0–20 min), followed by 5 min of washing and 10 min of reconditioning. Analyses of the samples (10.0 µL injected) were performed in an optimized DDA setting (272 nm) followed by MS/MS scans for the three most intense ions (Top 3). Three fixed collision energies were applied, 20, 40 and 60 V. MSMS acquisition parameters were as follows: *m/z* range 100-1700, default charge of 1, minimum intensity of 5000 counts, 3 spectra/s, isolation width: narrow mode (1.3 m/z). The negative

ESI mode conditions were set at a 2 GHz acquisition rate. Ionization source conditions were: drying gas temperature 320°C, drying gas flow rate 12 L/min, nebulizer 60 psig, fragmentor 120 V, skimmer 65 V. In the negative-ion mode, trifluoroacetic acid (TFA) anion $C_2O_2F_3$ $[M - H]^-$ ion (*m/z* 112.985587) and the TFA adduct of HP-0921 $C_{20}H_{18}O_8N_3P_3F_{27}$ $[M - H]^-$ ion (*m/z* 1033.988109) were used as internal lock masses. Full scans were acquired at a resolution of 11,000 (at *m/z* 1033).

5.5.3. MZmine 2 treatment and molecular networking

Data obtained from high resolution mass spectrometry were first processed with MZmine 2.51. The Agilent files were converted into mzXML format with the software MSconvert, part of the ProteoWizard package. After uploading into the MZmine workflow, the detection mass was performed with a noise level at 1.10^3 for MS^1 and 5.10^1 for MS^2. The chromatograms were built with the ADAP algorithm with a minimum group size of 2, a group intensity threshold of 1.10^3, a minimum highest intensity at 1.10^3 and an *m/z* tolerance at 20 ppm. The ADAP wavelet algorithm was then used for deconvolution with the following settings: S/N threshold: 2, S/N estimator: Intensity window SN, min feature height: 1000, coefficient/area threshold: 5, peak duration range: 0.01-7.00, RT wavelet range: 0.01-0.50. The *m/z* range for MS^2 scan pairing was set at 0.3 Da and the RT range at 1 min. The isotopic peak grouper algorithm was then used with an *m/z* tolerance at 20 ppm, an RT tolerance at 0.2 min and a maximum charge of 2. The peaks were aligned in a unique peak list using the join aligner algorithm with the following parameters: *m/z* tolerance: 20 ppm, weight for *m/z*: 1, retention time tolerance: 0.7, weight for RT: 1, require same charge state: unchecked, require same ID: unchecked. The gaps in the list were then filled with the algorithm “same RT and *m/z* range gap-filler” with an *m/z* tolerance at 20 ppm. Finally, the peak list was filtered using the peak list rows filter by keeping only the peaks with MS^2 scan (GNPS). The peak list was exported to a unique MGF file with a csv file gathering the metadata. The MGF file was imported into the GNPS platform (“GNPS - The Future of Natural Products Research and Mass Spectrometry,” n.d.; Wang et al., 2016).

A molecular network was created using the online workflow at GNPS (http://gnps.ucsd.edu). The data were filtered by removing all MS/MS peaks within +/- 17 Da of the precursor *m/z*. MS/MS spectra were window filtered by choosing only the top 6 peaks in the +/- 50 Da window throughout the spectrum. The molecular network was then created with a parent mass tolerance of 0.02 Da and an MS/MS fragment ion tolerance of 0.02 Da. The run MS cluster option was turned off. A network was then created where edges were filtered to have a cosine score above 0.7 and more than 6 matched peaks. Furthermore, edges between two nodes were kept in the network if and only if each of the nodes appeared in each other's respective top 10 most similar nodes. The spectra in the

network were then compared with GNPS' spectral libraries. The library spectra were filtered in the same manner as the input data. All matches kept between network spectra and library spectra were required to have a score above 0.7 and at least 4 matched peaks.

5.6. Synthesis of compound **H**

Synthesis was performed in accordance with the procedure previously published by Bazin et al., 2008 from ethanolamine (0.035 g, 0.6 mmol) and UA (0.200 g, 1 equiv). Column chromatography using CH_2Cl_2/EtOAc 90:10. Yellow solid; 78%. Rf = 0.30 (toluene/EtOAc 85:15); [α] = + 299°.dm^{-1}.g^{-1}.cm^3 (*c* 0.80, acetone); ^{1}H NMR (300 MHz, $CDCl_3$) δ 1.69 (CH_3-10), 2.08 (s, 3H, CH_3-15), 2.66 (s, 3H, CH_3-12), 2.66 (s, 3H, CH_3-14), 3.67 (m, 2H, H-a), 3.96 (m, 2H, H-b), 5.75 (s, 1H, H-4), 11.88 (bs, 1H, OH-9), 13.35 (s, 1H, OH-7); ^{13}C NMR (75 MHz, $CDCl_3$) δ 7.6 (CH_3-15), 18.7 (CH_3-12), 32.2 (CH_3-14), 32.2 (CH_3-10), 45.9 (C-a), 57.3 (C-9b), 60.6 (C-d), 101.5 (C-6), 102.5 (C-4), 102.6 (C-2), 105.1 (C-9a), 108.2 (C-8), 156.0 (C-6a), 158.3 (C-9), 163.7 (C-7), 174.3 (C-4a), 175.5 (C-11), 190.4 (C-3), 198.5 (C-1), 200.8 (C-13); HRMS (ESI) (*m/z*) calcd for $C_{20}H_{20}O_7N$ $[M-H]^-$ 386.12404; found 386.1226.

5.7. Antibacterial evaluation

All the strains of *Escherichia coli* (CIP 54.8T), *Pseudomonas aeruginosa* (CIP A22), *Staphyloccocus aureus* (CIP 53 156), *S. epidermidis* (CIP 53 124) and *Streptococcus agalactiae* (CIP 56.1) were provided by the Institut Pasteur. They were grown at 37°C using Luria Broth (LB) medium (2.5 g peptone, 2.5 g NaCl, 1.5 g yeast extract and 500 mL distilled water). The compounds were prepared in DMSO/methanol 50/50 at 2 mg/mL for UA and compound **H** and 10 mg/mL for gentamicin. According to the Clinical and Laboratory Standards Institute (CLSI) (National Committee for Clinical Laboratory Standards, 2004),the compounds were serially diluted 1:2 in LB in a sterile 96-well plate. Each well was then inoculated (excepted for compound controls) with 5 x 10^7 UFC/mL of each strain for 24 h at 37°C. The solvents used to prepare the compounds were also tested on the bacteria. All the wells were then plated on LB agar and incubated for 24 h at 37°C. Subsequently, the minimal inhibitory concentration (MIC), defined as the minimal concentration able to inhibit the visible bacterial growth, was determined as the clear well having the smallest concentration.

Acknowledgments

We sincerely thank Damien Olivier-Jimenez for his advice on data analysis and to Dr D. Delmail for the harvest of *P. hymenina*.

Funding declaration

This research did not receive any specific grant from funding agencies in the public, commercial, or not-for-profit sectors.

Appendix A. Supplementary Data.

Supplementary data to this article can be found online at https://

References:

Baqueiro-Peña, I., Contreras-Jácquez, V., Kirchmayr, M.R., Mateos-Díaz, J.C., Valenzuela-Soto, E.M., Asaff-Torres, A., 2019. Isolation and Characterization of a New Ferulic-Acid-Biotransforming Bacillus megaterium from Maize Alkaline Wastewater (Nejayote). Curr. Microbiol. 76, 1215–1224. https://doi.org/10.1007/s00284-019-01726-4

Bates, S.T., Cropsey, G.W.G., Caporaso, J.G., Knight, R., Fierer, N., 2011. Bacterial Communities Associated with the Lichen Symbiosis. Appl. Environ. Microbiol. 77, 1309–1314. https://doi.org/10.1128/AEM.02257-10

Bazin, M.-A., Lamer, A.-C.L., Delcros, J.-G., Rouaud, I., Uriac, P., Boustie, J., Corbel, J.-C., Tomasi, S., 2008. Synthesis and cytotoxic activities of usnic acid derivatives. Bioorg. Med. Chem. 16, 6860–6866. https://doi.org/10.1016/j.bmc.2008.05.069

Boufridi, A., Petek, S., Evanno, L., Beniddir, M.A., Debitus, C., Buisson, D., Poupon, E., 2016. Biotransformations versus chemical modifications: new cytotoxic analogs of marine sesquiterpene ilimaquinone. Tetrahedron Lett. 57, 4922–4925. https://doi.org/10.1016/j.tetlet.2016.09.075

Calcott, M.J., Ackerley, D.F., Knight, A., Keyzers, R.A., Owen, J.G., 2018. Secondary metabolism in the lichen symbiosis. Chem. Soc. Rev. 47, 1730–1760. https://doi.org/10.1039/C7CS00431A

Cardinale, M., Puglia, A.M., Grube, M., 2006. Molecular analysis of lichen-associated bacterial communities. FEMS Microbiol. Ecol. 57, 484–495. https://doi.org/10.1111/j.1574-6941.2006.00133.x

Cardinale, M., Vieira de Castro, J., Müller, H., Berg, G., Grube, M., 2008. In situ analysis of the bacterial community associated with the reindeer lichen Cladonia arbuscula reveals predominance of Alphaproteobacteria. FEMS Microbiol. Ecol. 66, 63–71. https://doi.org/10.1111/j.1574-6941.2008.00546.x

Choi, G., Gao, M., Lee, D.-S., Choi, H., 2017. Mabikibacter ruber gen. nov., sp. nov., a bacterium isolated from marine sediment, and proposal of Mabikibacteraceae fam. nov. in the class Alphaproteobacteria. Int. J. Syst. Evol. Microbiol. 67, 3375–3380. https://doi.org/10.1099/ijsem.0.002121

Cocchietto, M., Skert, N., Nimis, P., Sava, G., 2002. A review on usnic acid, an interesting natural compound. Naturwissenschaften 89, 137–146. https://doi.org/10.1007/s00114-002-0305-3

Francolini, I., Norris, P., Piozzi, A., Donelli, G., Stoodley, P., 2004. Usnic Acid, a Natural Antimicrobial Agent Able To Inhibit Bacterial Biofilm Formation on Polymer Surfaces. Antimicrob. Agents Chemother. 48, 4360–4365. https://doi.org/10.1128/AAC.48.11.4360-4365.2004

GNPS - The Future of Natural Products Research and Mass Spectrometry [WWW Document], n.d. URL https://gnps.ucsd.edu/ProteoSAFe/static/gnps-splash.jsp (accessed 3.20.18).

Goh, E.-B., Yim, G., Tsui, W., McClure, J., Surette, M.G., Davies, J., 2002. Transcriptional modulation of bacterial gene expression by subinhibitory concentrations of antibiotics. Proc. Natl. Acad. Sci. 99, 17025–17030.

Grube, M., Berg, G., 2009. Microbial consortia of bacteria and fungi with focus on the lichen symbiosis. Fungal Biol. Rev. 23, 72–85. https://doi.org/10.1016/j.fbr.2009.10.001
Grube, M., Cernava, T., Soh, J., Fuchs, S., Aschenbrenner, I., Lassek, C., Wegner, U., Becher, D., Riedel, K., Sensen, C.W., Berg, G., 2015. Exploring functional contexts of symbiotic sustain within lichen-associated bacteria by comparative omics. ISME J. 9, 412–424. https://doi.org/10.1038/ismej.2014.138
Hawksworth, D.L., Grube, M., 2020. Lichens redefined as complex ecosystems. New Phytol.
Jackson, E., Ripoll, M., Betancor, L., 2019. Efficient glycerol transformation by resting *Gluconobacter* cells. MicrobiologyOpen. https://doi.org/10.1002/mbo3.926
Kim, O.-S., Cho, Y.-J., Lee, K., Yoon, S.-H., Kim, M., Na, H., Park, S.-C., Jeon, Y.S., Lee, J.-H., Yi, H., Won, S., Chun, J., 2012. Introducing EzTaxon-e: a prokaryotic 16S rRNA gene sequence database with phylotypes that represent uncultured species. Int. J. Syst. Evol. Microbiol. 62, 716–721. https://doi.org/10.1099/ijs.0.038075-0
Lauterwein, M., Oethinger, M., Belsner, K., Peters, T., Marre, R., 1995. In vitro activities of the lichen secondary metabolites vulpinic acid, (+)-usnic acid, and (-)-usnic acid against aerobic and anaerobic microorganisms. Antimicrob. Agents Chemother. 39, 2541–2543.
Le Pogam, P., Le Lamer, A.-C., Legouin, B., Boustie, J., Rondeau, D., 2016. In situ DART-MS as a Versatile and Rapid Dereplication Tool in Lichenology: Chemical Fingerprinting of Ophioparma ventosa. Phytochem. Anal. 27, 354–363. https://doi.org/10.1002/pca.2635
Luziatelli, F., Brunetti, L., Ficca, A.G., Ruzzi, M., 2019. Maximizing the Efficiency of Vanillin Production by Biocatalyst Enhancement and Process Optimization. Front. Bioeng. Biotechnol. 7. https://doi.org/10.3389/fbioe.2019.00279
Luzina, O.A., Salakhutdinov, N.F., 2018. Usnic acid and its derivatives for pharmaceutical use: a patent review (2000–2017). Expert Opin. Ther. Pat. 28, 477–491. https://doi.org/10.1080/13543776.2018.1472239
Maciąg-Dorszyńska, M., Węgrzyn, G., Guzow-Krzemińska, B., 2014. Antibacterial activity of lichen secondary metabolite usnic acid is primarily caused by inhibition of RNA and DNA synthesis. FEMS Microbiol. Lett. 353, 57–62. https://doi.org/10.1111/1574-6968.12409
Martin, J.F., Demain, A.L., 1980. Control of antibiotic biosynthesis. Microbiol. Rev. 44, 230–251.
Martins, M.B., Carvalho, I., 2007. Diketopiperazines: biological activity and synthesis. Tetrahedron 63, 9923–9932. https://doi.org/10.1016/j.tet.2007.04.105
Millot, M., Dieu, A., Tomasi, S., 2016. Dibenzofurans and derivatives from lichens and ascomycetes. Nat. Prod. Rep. 33, 801–811. https://doi.org/10.1039/C5NP00134J
Millot, M., Tomasi, S., Studzinska, E., Rouaud, I., Boustie, J., 2009. Cytotoxic Constituents of the Lichen *Diploicia canescens*. J. Nat. Prod. 72, 2177–2180. https://doi.org/10.1021/np9003728
Nahar, S., Jeong, M.-H., Hur, J.-S., 2019. Lichen-Associated Bacterium, a Novel Bioresource of Polyhydroxyalkanoate (PHA) Production and Simultaneous Degradation of Naphthalene and Anthracene. J. Microbiol. Biotechnol. 29, 79–90. https://doi.org/10.4014/jmb.1808.08037
National Committee for Clinical Laboratory Standards, 2004. Methods for Antimicrobial Susceptibility Testing of Anaerobic Bacteria: Approved Standard, 6th edition, Wayne Pa.: NCCLS. ed.
Noël, A., Ferron, S., Rouaud, I., Gouault, N., Hurvois, J.-P., Tomasi, S., 2017. Isolation and Structure Identification of Novel Brominated Diketopiperazines from Nocardia ignorata—A Lichen-Associated Actinobacterium. Molecules 22, 371. https://doi.org/10.3390/molecules22030371
Olivier-Jimenez, D., Chollet-Krugler, M., Rondeau, D., Beniddir, M.A., Ferron, S., Delhaye, T., Allard, P.-M., Wolfender, J.-L., Sipman, H.J.M., Lücking, R., Boustie, J., Le Pogam, P., 2019. A database of high-resolution MS/MS spectra for lichen metabolites. Sci. Data 6. https://doi.org/10.1038/s41597-019-0305-1
Parrot, D., Antony-Babu, S., Intertaglia, L., Grube, M., Tomasi, S., Suzuki, M.T., 2015a. Littoral lichens as a novel source of potentially bioactive Actinobacteria. Sci. Rep. 5, 15839. https://doi.org/10.1038/srep15839

Parrot, D., Intertaglia, L., Jehan, P., Grube, M., Suzuki, M.T., Tomasi, S., 2018. Chemical analysis of the Alphaproteobacterium strain MOLA1416 associated with the marine lichen Lichina pygmaea. Phytochemistry 145, 57–67. https://doi.org/10.1016/j.phytochem.2017.10.005

Parrot, D., Legrave, N., Intertaglia, L., Rouaud, I., Legembre, P., Grube, M., Suzuki, M.T., Tomasi, S., 2016. Cyaneodimycin, a Bioactive Compound Isolated from the Culture of *Streptomyces cyaneofuscatus* Associated with *Lichina confinis*. Eur. J. Org. Chem. 2016, 3977–3982. https://doi.org/10.1002/ejoc.201600252

Parrot, D., Peresse, T., Hitti, E., Carrie, D., Grube, M., Tomasi, S., 2015b. Qualitative and Spatial Metabolite Profiling of Lichens by a LC-MS Approach Combined With Optimised Extraction: Metabolite Profiling by lc-ms of Lichens Combined With Optimized Extraction. Phytochem. Anal. 26, 23–33. https://doi.org/10.1002/pca.2532

Pluskal, T., Castillo, S., Villar-Briones, A., Orešič, M., 2010. MZmine 2: Modular framework for processing, visualizing, and analyzing mass spectrometry-based molecular profile data. BMC Bioinformatics 11, 395. https://doi.org/10.1186/1471-2105-11-395

Rice, K.C., Bayles, K.W., 2008. Molecular Control of Bacterial Death and Lysis. Microbiol. Mol. Biol. Rev. 72, 85–109. https://doi.org/10.1128/MMBR.00030-07

Robertson, S.M., Luo, X., Dubey, N., Li, C., Chavan, A.B., Gilmartin, G.S., Higgins, M., Mahnke, L., 2015. Clinical drug-drug interaction assessment of ivacaftor as a potential inhibitor of cytochrome P450 and P-glycoprotein. J. Clin. Pharmacol. 55, 56–62. https://doi.org/10.1002/jcph.377

Schmitt, I., Lumbsch, H.T., 2009. Ancient Horizontal Gene Transfer from Bacteria Enhances Biosynthetic Capabilities of Fungi. PLoS ONE 4, e4437. https://doi.org/10.1371/journal.pone.0004437

Sundset, M.A., Barboza, P.S., Green, T.K., Folkow, L.P., Blix, A.S., Mathiesen, S.D., 2010. Microbial degradation of usnic acid in the reindeer rumen. Naturwissenschaften 97, 273–278. https://doi.org/10.1007/s00114-009-0639-1

Suzuki, M.T., Parrot, D., Berg, G., Grube, M., Tomasi, S., 2016. Lichens as natural sources of biotechnologically relevant bacteria.. Appl. Microbiol. Biotechnol. 100 (2), 583–595. doi:10.1007/s00253-015-7114-z.

Taguchi, H., Sankawa, U., Shibata, S., 1969. Biosynthesis of Natural Products. VI. Biosynthesis of Usnic Acid in Lichens. A General Scheme of Biosynthesis of Usnic Acid. Chem. Pharm. Bull. (Tokyo) 17, 2054–2060. https://doi.org/10.1248/cpb.17.2054

Tahlan, K., Yu, Z., Xu, Y., Davidson, A.R., Nodwell, J.R., 2008. Ligand Recognition by ActR, a TetR-Like Regulator of Actinorhodin Export. J. Mol. Biol. 383, 753–761. https://doi.org/10.1016/j.jmb.2008.08.081

Wang, M., Carver, J.J., Phelan, V.V., Sanchez, L.M., Garg, N., Peng, Y., Nguyen, D.D., Watrous, J., Kapono, C.A., Luzzatto-Knaan, T., Porto, C., Bouslimani, A., Melnik, A.V., Meehan, M.J., Liu, W.-T., Crüsemann, M., Boudreau, P.D., Esquenazi, E., Sandoval-Calderón, M., Kersten, R.D., Pace, L.A., Quinn, R.A., Duncan, K.R., Hsu, C.-C., Floros, D.J., Gavilan, R.G., Kleigrewe, K., Northen, T., Dutton, R.J., Parrot, D., Carlson, E.E., Aigle, B., Michelsen, C.F., Jelsbak, L., Sohlenkamp, C., Pevzner, P., Edlund, A., McLean, J., Piel, J., Murphy, B.T., Gerwick, L., Liaw, C.-C., Yang, Y.-L., Humpf, H.-U., Maansson, M., Keyzers, R.A., Sims, A.C., Johnson, A.R., Sidebottom, A.M., Sedio, B.E., Klitgaard, A., Larson, C.B., Boya P, C.A., Torres-Mendoza, D., Gonzalez, D.J., Silva, D.B., Marques, L.M., Demarque, D.P., Pociute, E., O'Neill, E.C., Briand, E., Helfrich, E.J.N., Granatosky, E.A., Glukhov, E., Ryffel, F., Houson, H., Mohimani, H., Kharbush, J.J., Zeng, Y., Vorholt, J.A., Kurita, K.L., Charusanti, P., McPhail, K.L., Nielsen, K.F., Vuong, L., Elfeki, M., Traxler, M.F., Engene, N., Koyama, N., Vining, O.B., Baric, R., Silva, R.R., Mascuch, S.J., Tomasi, S., Jenkins, S., Macherla, V., Hoffman, T., Agarwal, V., Williams, P.G., Dai, J., Neupane, R., Gurr, J., Rodríguez, A.M.C., Lamsa, A., Zhang, C., Dorrestein, K., Duggan, B.M., Almaliti, J., Allard, P.-M., Phapale, P., Nothias, L.-F., Alexandrov, T., Litaudon, M., Wolfender, J.-L., Kyle, J.E., Metz, T.O., Peryea, T., Nguyen, D.-T., VanLeer, D., Shinn, P., Jadhav, A., Müller, R., Waters, K.M., Shi, W., Liu, X., Zhang, L., Knight, R., Jensen, P.R., Palsson, B.Ø., Pogliano, K.,

Linington, R.G., Gutiérrez, M., Lopes, N.P., Gerwick, W.H., Moore, B.S., Dorrestein, P.C., Bandeira, N., 2016. Sharing and community curation of mass spectrometry data with Global Natural Products Social Molecular Networking. Nat. Biotechnol. 34, 828–837. https://doi.org/10.1038/nbt.3597

Zheng, K.-X., Jiang, Y., Jiang, J.-X., Huang, R., He, J., Wu, S.-H., 2019. A new phthalazinone derivative and a new isoflavonoid glycoside from lichen-associated Amycolatopsis sp. Fitoterapia 135, 85–89. https://doi.org/10.1016/j.fitote.2019.04.011

Zhou, J., Xiong, X., Wang, K., Zou, L., Lv, D., Yin, Y., 2017. Ethanolamine Metabolism in the Mammalian Gastrointestinal Tract: Mechanisms, Patterns, and Importance. Curr. Mol. Med. 17. https://doi.org/10.2174/1566524017666170331161715

Figures and Tables:

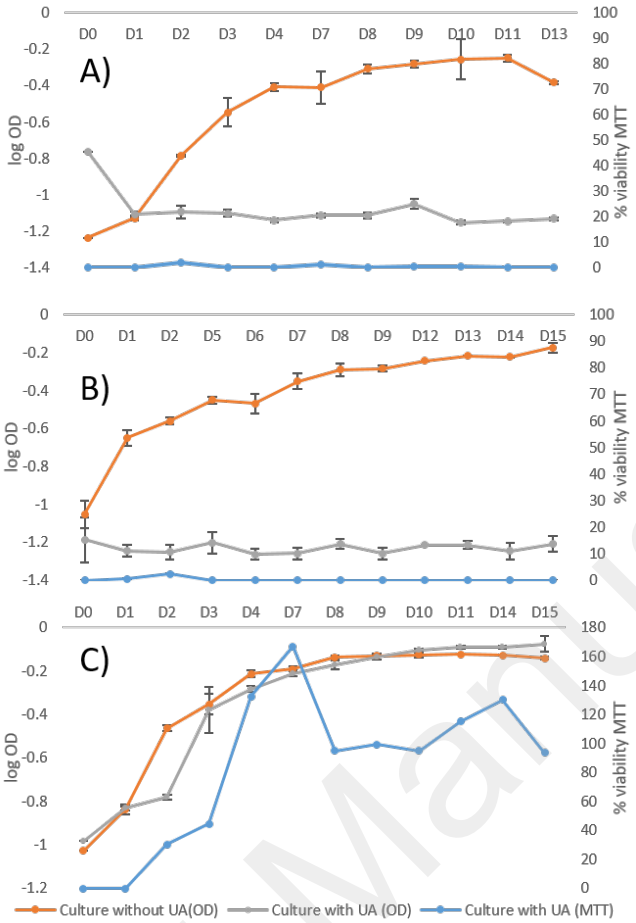

Fig. 1. Monitoring of the bacterial growth over 15 days (D0 to D15) by measuring optical density (log OD (optical density), gray curve) and cell viability (%) using MTT assay (blue curve) compared to untreated culture (orange curve). A) *Nocardia* sp., B) *S. cyaneofuscatus*, C) *M. ruber*.

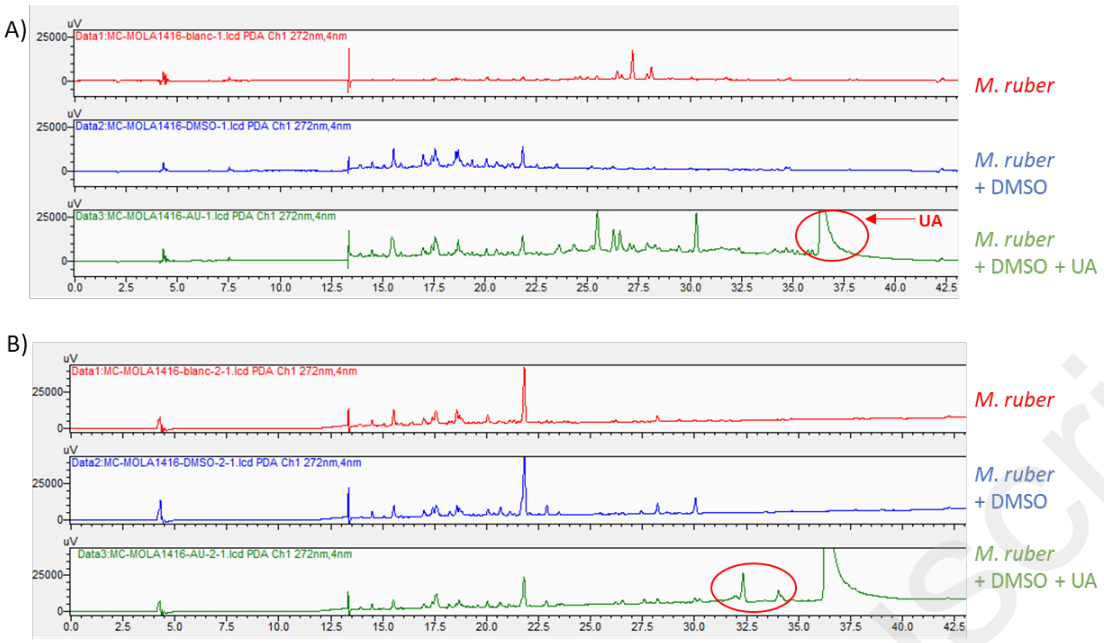

Fig. 2. HPLC chromatograms of *M. ruber* cultures with or without UA. A) At the beginning of the stationary phase of bacterial growth; B) After 7 days of stationary phase. Compounds circled in red appear only in the culture with UA.

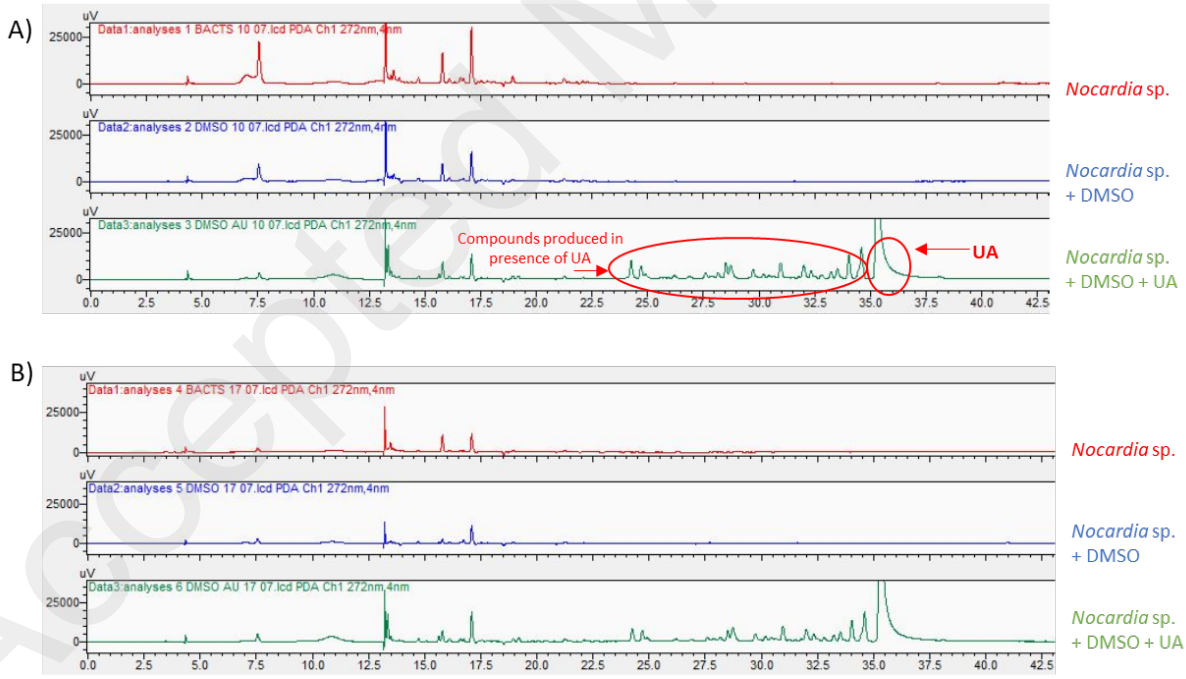

Fig. 3. HPLC chromatograms of *Nocardia* sp. culture with or without UA. A) At the beginning of the stationary phase of the bacterial growth; B) After 7 days of stationary phase. Compounds circled in red appear only in the culture with UA.

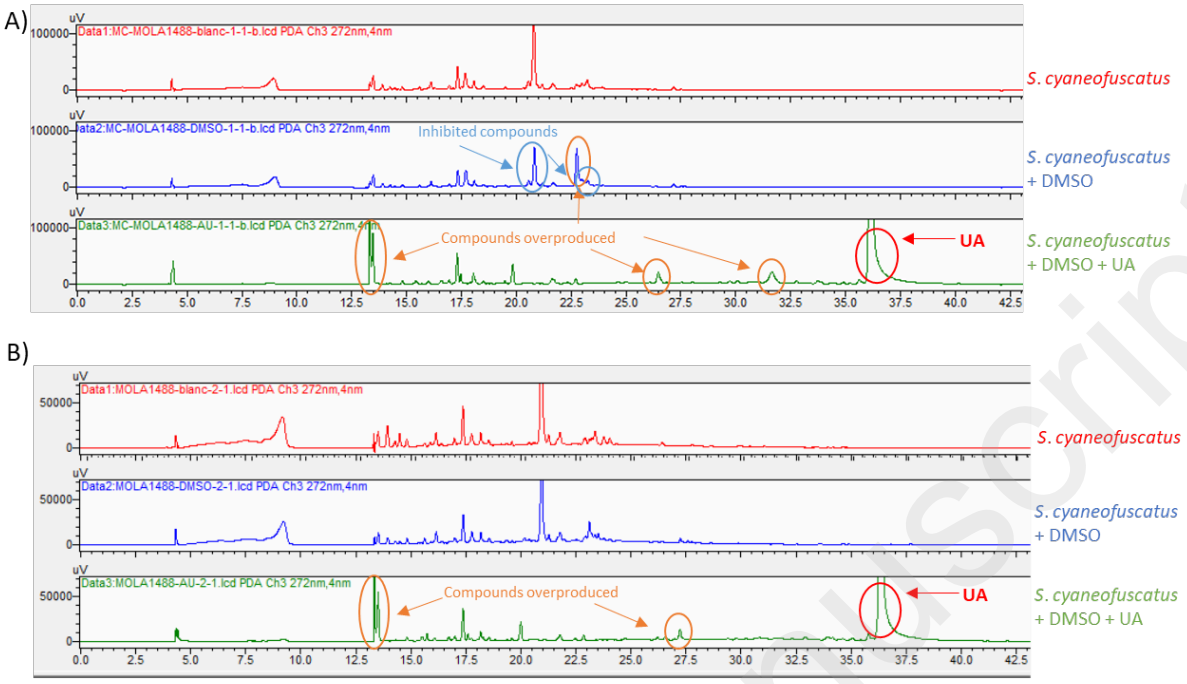

Fig. 4. HPLC chromatograms of *S. cyaneofuscatus* cultures with or without UA: A) At the beginning of the stationary phase of bacterial growth; B) After 7 days of stationary phase. Circled in blue: compounds inhibited in the presence of UA, circled in orange: compounds more concentrated in the presence of UA, circled in red: UA.

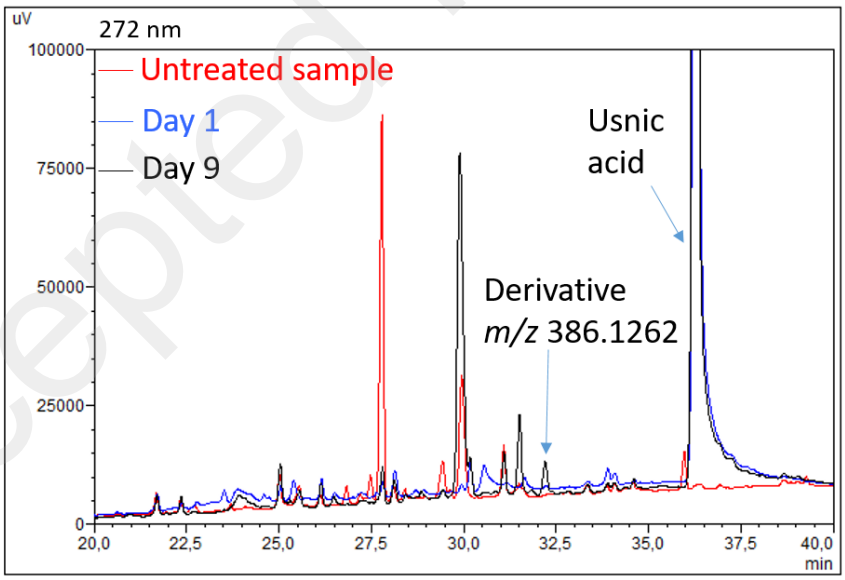

Fig. 5. Comparison of HPLC chromatograms of *B. weihenstephanensis* extracts with UA at 0.01 mg/mL after 1 day of culture (blue), 9 days of culture (black) and without UA after 9 days of culture (red).

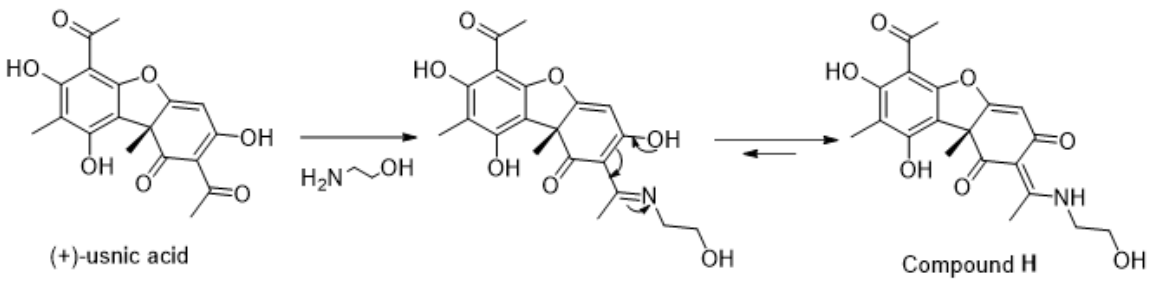

Fig. 6. UA and the ethanolamine **H** derivative obtained after biotransformation

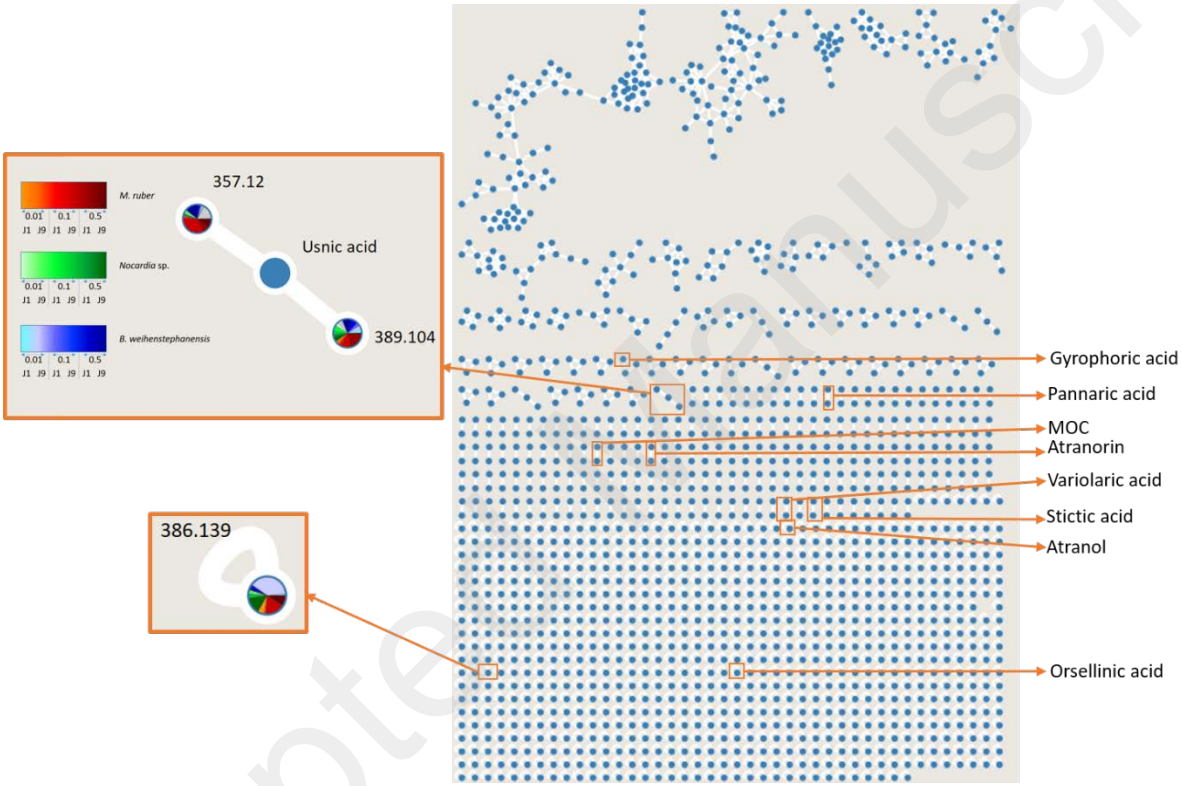

Fig. 7. Molecular networking results from GNPS visualized with Cytoscape. Inset: cluster of UA and derivatives with close fragmentation pathway (*m/z* 357.12: compound **K**, *m/z* 389.104: compound **L**) and self-loop of compound **H** (at *m/z* 386.139).

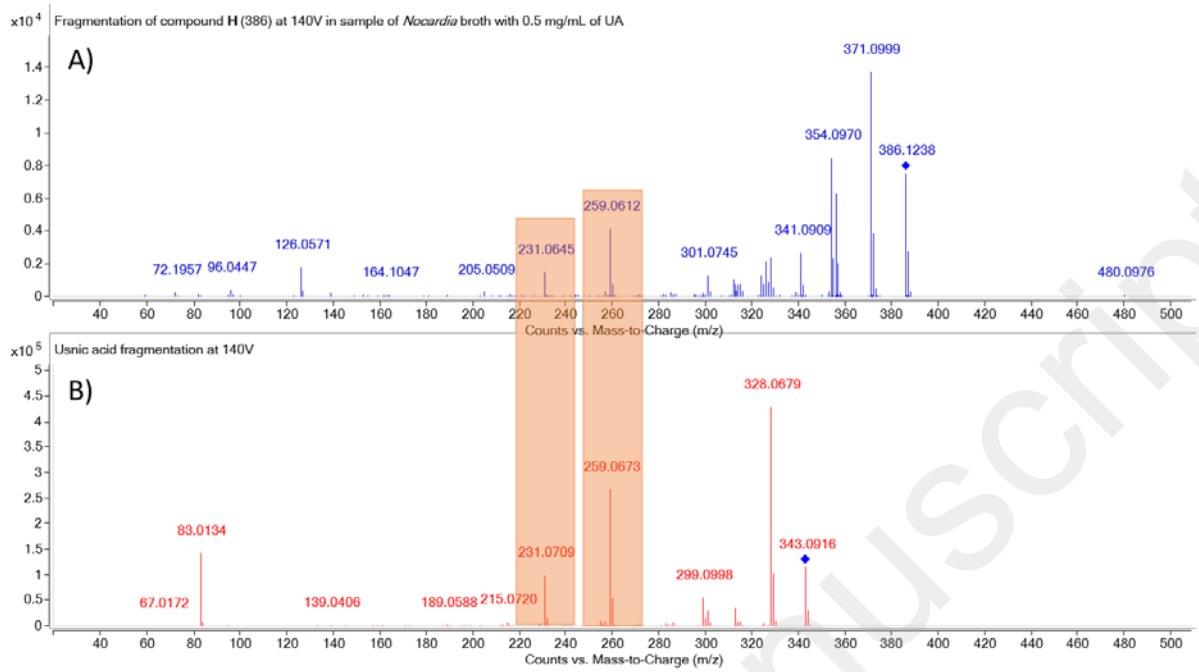

Fig. 8. Fragmentation patterns in negative mode of A) compound **H** and B) UA; common fragments are highlighted in orange.

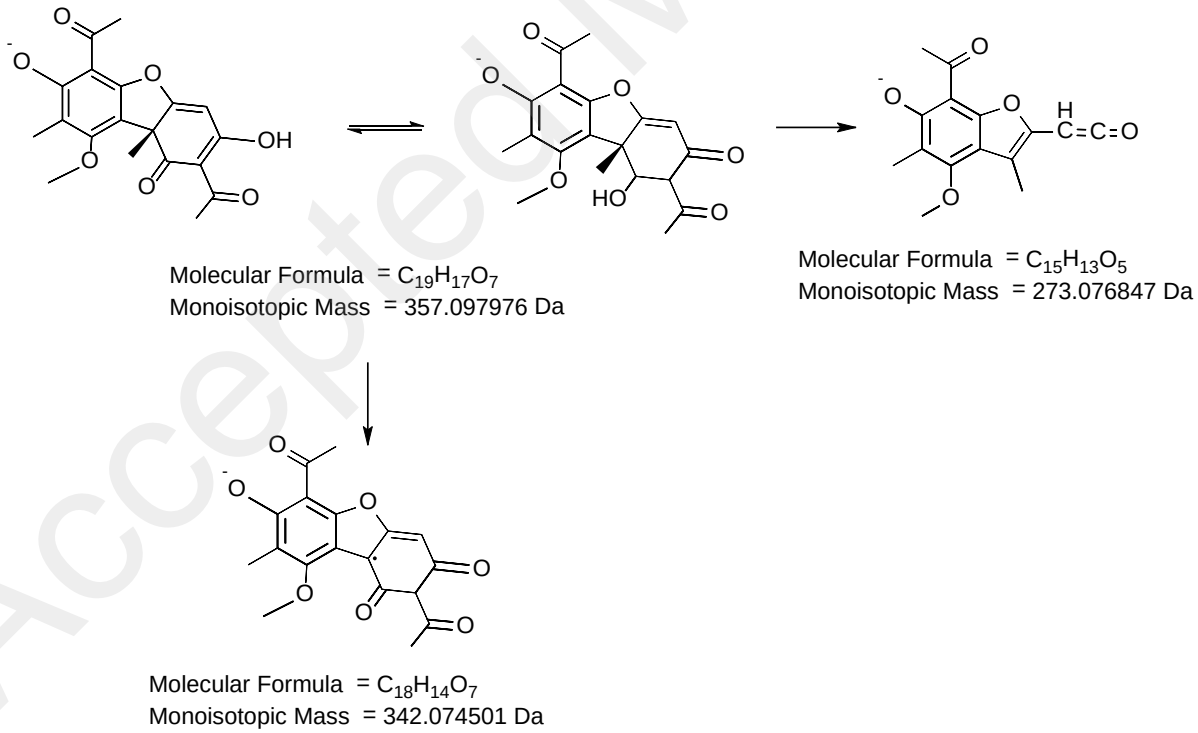

Fig. 9. Fragmentation pattern proposed for one possible isomer of the methylated usnic acid **K**

Table 1 Additional peaks detected only in cultures treated with UA at different concentrations (0.01 to 0.5 mg/mL)

Peak, retention time (min)	Bacterial strain and (+)-usnic acid concentration (mg/mL)								
	M. ruber			***Nocardia* sp.**			***B. weihenstephenensis***		
	0.01	**0.1**	**0.5**	**0.01**	**0.1**	**0.5**	**0.01**	**0.1**	**0.5**
A: 22.8	-	-	-	-	-	+↑	-	-	-
B: 23.7	-	-	-	-	+↑	+	-	-	-
C: 26.6	-	-	-	+	+↑	+	+	-	+↑
D: 28.4	-	-	-	-	-	-	+	-	-
E: 30.2	-	-	+↑	+	+	+	+↑	+	+↑
F: 30.6	-	-	-	-	-	-	+	+	+
G: 32.1	-	-	-	-	-	+↑	-	-	-
H: 32.4	+↑	+↑	+↑	-	-	+	+↑	-	-
I: 34.2	-	-	-	+	+	+	+	+↑	+
J: 36.4	-	-	-	+	+	+	-	-	-

+: detected; ↑ : increase of peak height (at 272 nm) of compounds between 1 and 9 culture days.

Table 2 Antibacterial evaluation of UA and compound **H** against six pathogenic human bacterial strains

	(+)-Usnic acid	Compound H	Gentamicin
Strains	**MIC (µg/mL)**		
Escherichia coli (CIP 54.8T)	-	-	0.49
Pseudomonas aeruginosa (CIP A22)	-	-	0.98
Staphylococcus aureus (CIP 53 156)	6.25	50	0.98
Staphylococcus epidermidis (CIP 53 124)	1.56	50	31.20
Streptococcus agalactiae (CIP 56.1)	1.56	50	0.12